Nat.Volatiles&Essent.Oils,2021;8(4): 9326-9339

Modelling and Simulation of Multiple Permanent Magnet Synchronous Generators Based Wecs with Dc Voltage Regulation

[1]Ashwini Sugirayyanamath, [2]Dr. G V Jayaramaiah

[1]Mtech, Power electronics, Dr Ambedkar Institute of Technology, Malathahalli, Bengaluru-560056

[2] Professor and HOD, Electrical and Electronics Engineering, Dr Ambedkar Institute of Technology, Malathahalli, Bengaluru-560056

Abstract

In this, three wind turbine driven Permanent Magnet Synchronous Generators are modelled and simulated. The proposed system is tested with dc loads of different power ratings. The machine side controller is designed to obtain theMPPT control (Maximum Power Point Tracking) so that the wind power was extracted, whereas the load side controller provides the DC voltage regulation for the connected loads. Simulation work is carried out using Matlab/Simulink.

Index Terms— Voltage mode control, Buck converter, PMSG (Permanent Magnet Synchronous Generator).

1. Introduction

Recently, the renewable energy sources are shown interest as they are free from pollution, no requirement of raw fuels such as coal, diesel, etc., Especially the wind energy is in much demand as it is perennial resource for energy generation. This leads to generation of electrical energy from wind energy under controlled environment to achieve better performance in terms of electrical quantities like frequency, power and voltage. The generated power is either fed to the grid based on the grid requirements and remaining power is stored in the storage devices such as batteries for later consumption. There are two types of induction generators, SCIG and DFIG which is used for fixed speed wind energy conversion systems. There is need for variable speed generators as the wind speed is continuously varying. Also, the requirement of generators to operate in grid connected mode and also for standalone mode are increasing. The PMSGs are now used for fulfil those requirements providing generation of electrical power from wind energy as shown in Fig 1. In such scenarios, an storage element such as battery is introduced as it provides stability to the system in low wind speed.

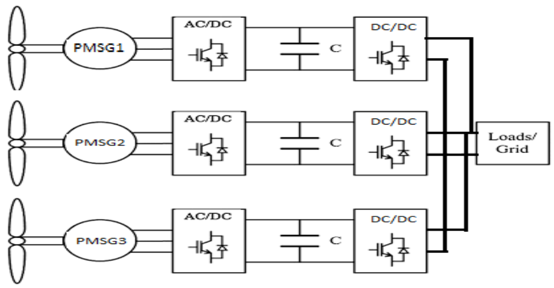

Fig 1 Proposed System of Wind Energy Conversion

In case of grid connected mode, the battery is unnecessary as it can be fed to the grid directly while maintaining the voltage and frequency as constant.

II. Modelling of Wind Turbine

The wind turbine process the energy from the wind to mechanical energy and later it is converted as electrical energy in the hands of electrical generator [1].The power generated by the wind turbine with area *A*, is provided below [2]:

$$P_m = \frac{1}{2}\rho A V^3 C_p(\lambda, \beta) \qquad (1)$$

where

ρ - air density(kg/m3),

P_m-power generated using wind (watts or J/s),

A-swept area of the blades of the turbine (m^2),

V-velocity of the wind (m/s) and

C_p-coefficient of power [3] [4] [5] [6]:

$$\lambda = \frac{\omega_m . R}{v} \qquad (2)$$

where

ω_m–speed of the rotor of electrical generator (rad/s),

R- radius of swept area and

β- pitch angle (degrees).

The coefficient of power is provided below (3):

$$C_p(\lambda,\beta) = C_1\left(\frac{C_2}{\lambda_i} - C_3\beta - C_4\right)e^{\frac{-C_5}{\lambda_i}} + C_6\lambda \tag{3}$$

And

$$\lambda_i = \frac{1}{\left(\frac{1}{\lambda + 0.08\beta} - \frac{0.035}{\beta^3 + 1}\right)} \tag{4}$$

The parameters of power coefficients of (3) are:

$C_1 = 0.5176$,
$C_2 = 116$,
$C_3 = 0.4$,
$C_4 = 5$,
$C_5 = 21$ and
$C_6 = 0.0068$

The maximum coefficient of power is 0.593 which denotes that we can achieve the maximum efficiency of 59.3% as the power extracted by the wind turbine is within 59.3%. In practical, due to various inefficiencies and losses due to aerodynamics of the turbine the actual coefficients of power arenearly 40 %. In Fig 2, the performance of the wind turbine is provided by the graph between coefficient of power and tip speed ratio for various pitch angles. It is observed as the maximum value of coefficient of power is 0.48 for λ =8.1 with pitch angle, β = 0.

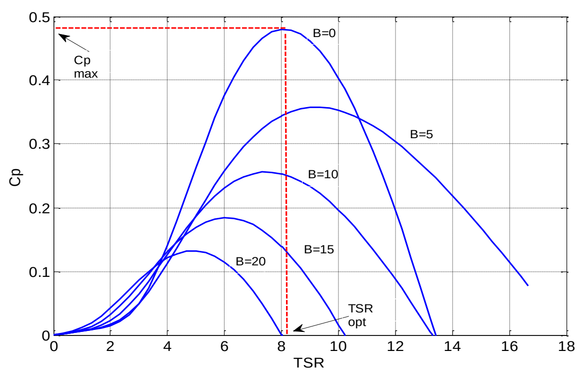

Fig. 2 Variation of power coefficient with TSR for different pitch angle

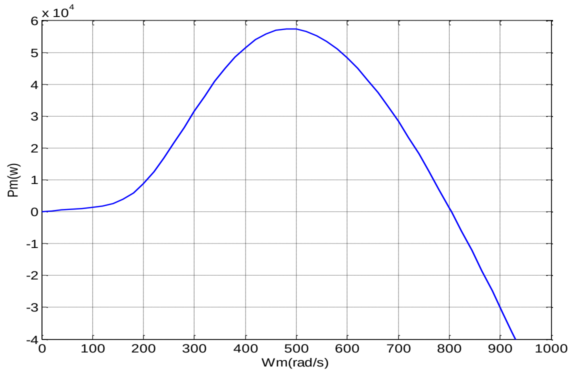

Fig. 3 Po vs ω

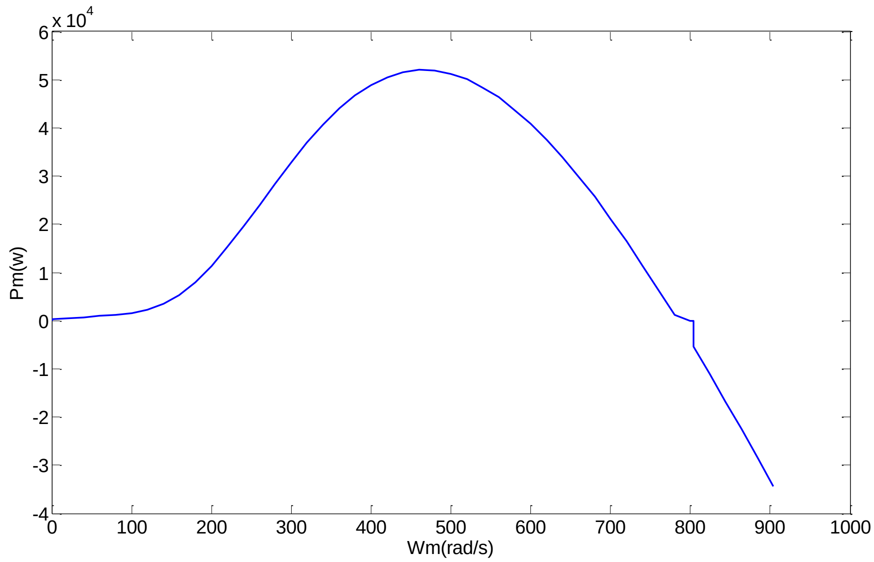

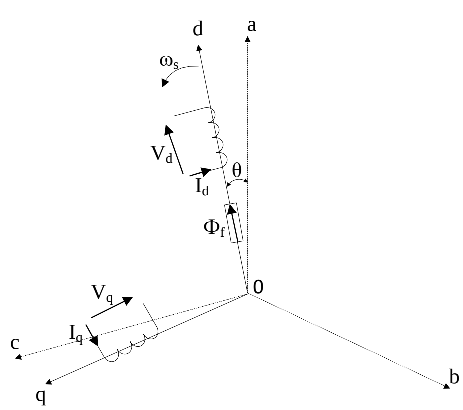

Fig. 4 dq and abc axis of PMSG model

III. PMSG Models

In the PMSG modelling, the q axis is leading by 90 degrees with d axis in the synchronous rotation frame. The abc and d-q axis of PMSG is shown in Fig 4. The equations of *d-q* voltages of the electrical generator are provided by (5) and (6) [7], [8]:

$$v_{gd} = R_g i_d + L_d \frac{di_d}{dt} + \frac{d\psi_f}{dt} - \omega_e L_q i_q \tag{5}$$

$$v_{gq} = R_g i_q + L_q \frac{di_q}{dt} + \frac{d\psi_f}{dt} + \omega_e (L_d i_d + \psi_f) \tag{6}$$

The speed of the rotatingelectrical field of the PMSG provided in [9]:

$$\omega_e = (p_n / 2)\omega_m \tag{7}$$

The *d* and *q*parameters are acquired from abc parameters using Park's transformationis provided below in (8):

$$\begin{bmatrix} V_d \\ V_q \\ V_0 \end{bmatrix} = \frac{2}{3} \begin{bmatrix} \sin\omega t & \sin(\omega t - 2\pi/3) & \sin(\omega t + 2\pi/3) \\ \cos\omega t & \cos(\omega t - 2\pi/3) & \cos(\omega t - 2\pi/3) \\ 1/2 & 1/2 & 1/2 \end{bmatrix} \begin{bmatrix} V_a \\ V_b \\ V_c \end{bmatrix} \tag{8}$$

Similarly, the abc parameters are acquired from the d*q*parametersusing Inverse Park's transformation is provided below:

$$\begin{bmatrix} V_a \\ V_b \\ V_c \end{bmatrix} = \begin{bmatrix} \sin\omega t & \cos\omega t & 1 \\ \sin(\omega t - 2\pi/3) & \cos(\omega t - 2\pi/3) & 1 \\ \sin(\omega t + 2\pi/3) & \cos(\omega t + 2\pi/3 & 1 \end{bmatrix} \begin{bmatrix} V_d \\ V_q \\ V_0 \end{bmatrix} \tag{9}$$

The input power that is measuredin the stator side is provided in (10):

$$P_{in} = V_{sa} i_a + V_{sb} i_b + V_{sc} i_c \tag{10}$$

where V_{sa} , V_{sb} , V_{sc} are voltages across the stator windings.

The power can be described in terms of dq parameters are provided below in (11):

$$P_{in} = \frac{3}{2}(V_d i_d + V_q i_q) \tag{11}$$

The resultant power is provided in (12):

$$P_{out} = \frac{3}{2}(\omega_r L_d i_d i_q + \omega_r \psi_m i_q - \omega_r L_q i_q i_d) \tag{12}$$

The resultant power is provided in (13) with pole pairs *as*:

$$P_{out} = \frac{3}{4} p_n \omega_m (L_d i_d i_q + \psi_m i_q - L_q i_q i_d) \quad (13)$$

The torque (T_e) equation can be expressed from eq 13 by dividing it with rotor speed is provided in (14):

$$T_e = \frac{3}{4} p_n (L_d i_d i_q + \psi_m i_q - L_q i_q i_d) \quad (14)$$

The electromagnetic torque is provided below in (15) with pole pairs (p):

$$T_e = \frac{3}{2} p((L_d - L_q) i_d i_q + \psi_m i_q) \quad (15)$$

IfL_d= L_q, and the torque equation is provided below in (16) as:

$$T_e = \frac{3}{2} p_n \psi_f i_q \quad (16)$$

The wind turbine dynamic equation is provided in (17):

$$J \frac{d\omega_m}{dt} = T_e - T_m - F\omega_m \quad (17)$$

where J is the inertia moment, F is the coefficient of viscous friction and T_m is torque transferred from the wind turbine.

1. Buck Converter

The buck converter circuit is provided in Fig. 5.

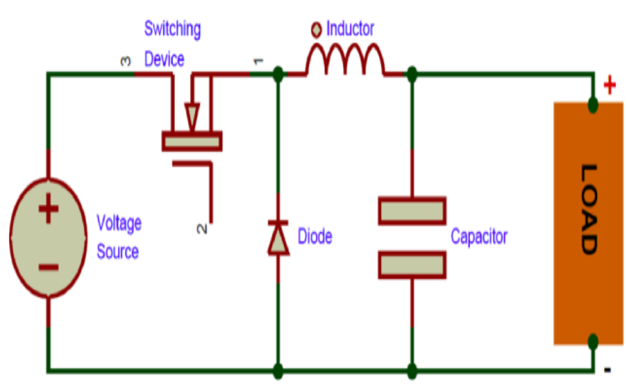

Fig 5 Buck Converter Circuit

The buck converter is used to step-down the dc voltage according to the duty ratio of the switching pulse provided. It consists of an inductor, switch, diode and capacitor. The load voltage will be less than that of input voltage. The operational stages of the buck converter are provided as follows:

Stage A

The operational circuit of buck converter in stage Ais provided in Fig. 6. Here, the gate pulse provided to switch S is HIGH and the inductor gets charged during this time period. The inductor voltage and load voltage are provided in the following equations:

$$V_o = V_{in} - V_L$$

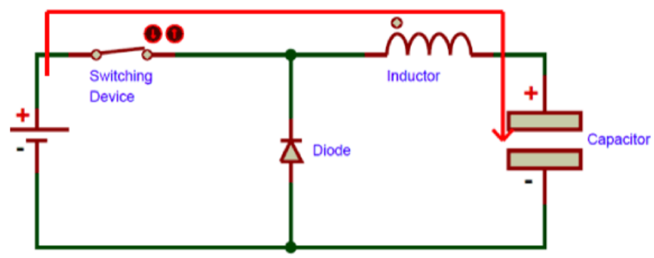

Fig 6 Stage A operational Circuit of Buck Converter, Vo=Vin-V_L

STAGE B

The operational circuit of the buck converter in stageB is provided in Fig. 7. Here, the gating pulse provided for the switch, S is LOW and the inductor gets discharged during this time period. The load voltage is provided in the following equation:

$$V_o = V_L$$

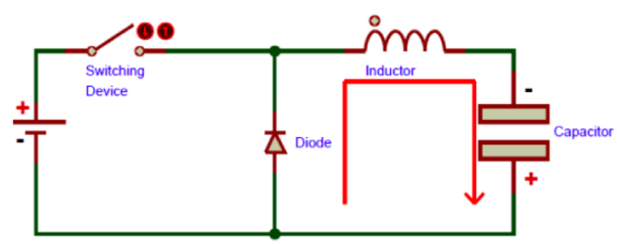

Fig 7 Stage B Operational Circuit of Buck Converter, Vo=V_L

The design of the buck converter circuit is provided by the following equations:

The Duty ratio (D) of the buck converter circuit is provided below:

$$D = \frac{Vo}{Vin}$$

The inductor value of the buck converter circuit is calculated by the following equation:

$$L = \frac{Vo*(Vo\text{-}Vin)}{\Delta Io*Fsw*Vin}$$

The inductor ripple current is selected using the following equation:

$$\Delta I_L = 0.2 * I_{in}$$

The output capacitance of the buck converter circuit is given by the following equation:

$$Co = \frac{\Delta Ioc}{8*Fsw*\Delta Vo}$$

The capacitor ripple voltage is selected from the following equation:

$$\Delta Voc = 2\%\ of Vo$$

1. Proposed Control Schemes

In this, the frequency and voltage is to be maintained as constant and hence the generator side and load side controllers are designed in such a way to achieve this.

A. Generator Side Controller(GSC)

In this, the controller consists of two loops named as outer and inner loops. In outer loop, the rotor speed is controlled with the help of PI controller whereas in the inner loops, direct and quadrature axis current are being controlled with separate PI controllers. From 16, the torque is being in phase with quadrature axis current and hence using q axis current, the torque control is achieved.

The PI controller consists of a proportional constantK_P and integrator constantK_I, which is tuned in order to achieve the control and better response. The reference q-axis current i_{qref} is provided by speed control loop and the PI controller output is:

$$i_{qref} = K_{p\omega} e_{\omega} + K_{I\omega} \int e_{\omega} dt \qquad (18)$$

The *d-q* output voltage from the PI controller areprovided below:

$$V^*{}_d = K_{pi} e_d + K_{Ii} \int e_d dt - \omega_r L_q i_q \qquad (19)$$

$$V^*{}_q = K_{pi} e_q + K_{Ii} \int e_q dt + \omega_r (L_d i_d + \phi_m) \qquad (20)$$

The *Vd** and *Vq** are transformed to three phase *abc* voltages by inverse Park transformation to 3 phasemodulation signals which is provided to PWM in order to generate pulses for the generator side converter.

B. Load Side Converter Control(LSC)

The proposed voltage mode controller block diagram is shown in Fig 8. The reference voltage compared with the measured voltage and the error voltage generated is provided to PI controller. The PI controller provides the duty ratio for buck converter so that the error voltage is to be reduced and reached zero.

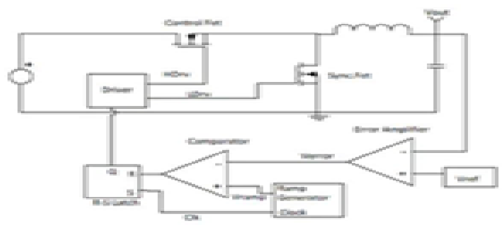

Fig 8 Constant Voltage Control Circuit for Buck Converter

The transfer function of PI controller is provided below:

Gpi(s) = K_p+ K_i/S

Design of Ann Control

The ANN senses the change in voltage and power and generates the duty ratios as per the equations (2) and (3). Hence if there is change in irradiation, the ANN control is accurate and quicker in response than any other control and provides the appropriate duty ratio in order to extract maximum PV power. The training was done with the help of data taken from the base system. The Levenberg-Marquardt algorithm used for training the neural network. This algorithm requires more memory but minimum time. Training will stop when improvement of generalization stops, as indicated by an increase in the mean square error of the validation samples.

The fitting curve of the training of ANN controller is provided in the following graphs (Fig. 9):

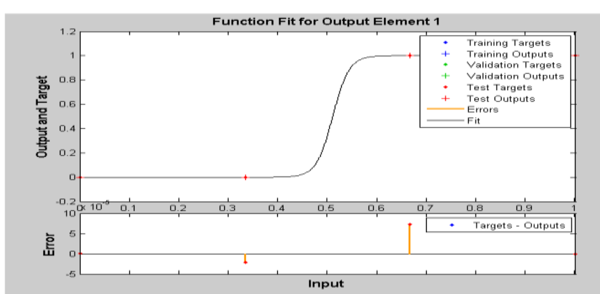

Fig 9 Fitting Curves from Neural Network Training

The regression value obtained from the training of neural network control is 0.99953. The regression curve is provided in the following graphs (Fig 10):

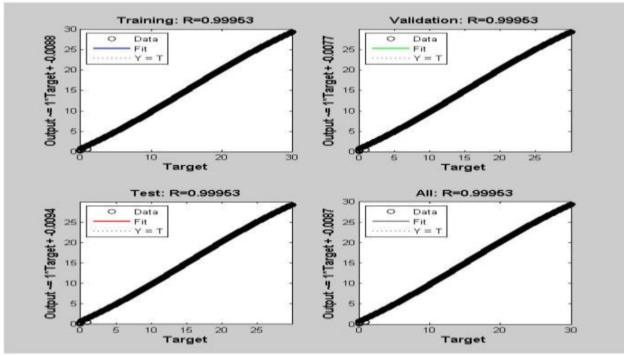

Fig 10 Regression Curves from Neural Network Training

1. Simulation and Results

The simulation data is provided below in Table I.

Table I

Wind Turbine Generator System Parameters

Wind Turbine Parameters	
Turbine Blade Radius (R)	6 m
Air Density (ρ)	1.11
Nominal wind velocity V_{wind}	12 m/s
Maximum value of power coefficient (C_p)	0.48
Optimum value of Tip speed ratio (λ)	8.1
PMSG parameters	
Stator winding resister (R_s)	0.25 Ω
Stator winding inductance (L_q=L_d=L)	0.6857 mH
Permanent flux	0.0534 Wb
pole pairs (p)	24
Moment of inertia (J)	0.0001295 Kg.m^3
Coefficient of viscous friction (F)	0.0001 N.m.s
DC Link	
DC link Voltage	760 V
Capacitor (C)	2.2 mF
Inductor (L)	0.5 mH

The simulation circuit is provided below in Fig 11

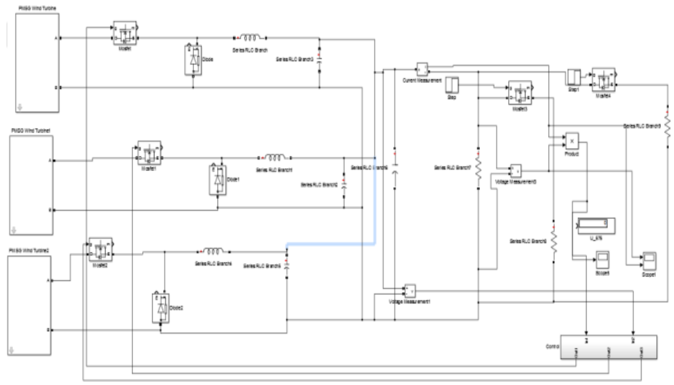

Fig 11 Simulation Circuit of Proposed WECS

In this, three wind energy conversion system with PMSG provides supply to the load using three set of machine side converter and buck converter. Initially Load1 is connected to the system and after t=1s, load2 is connected and again at t=2s, load3 is connected. By this, the transient and steady state performance of the proposed control system is verified. The wind speed is provided as 12m/s. The rotor speed of the PMSG is provided below along with reference speed in Fig 12.

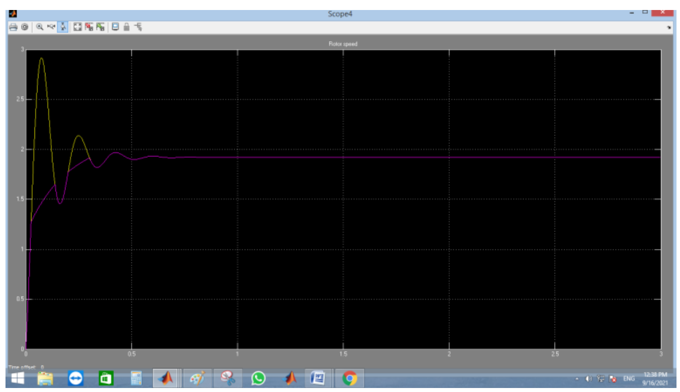

Fig 12 Reference and Actual Rotor Speed of PMSG

In this, initially there are oscillations present in the waveforms and it is settled within 0.4s and the actual rotor speed is controlled by the reference speed provided to the controller.

The stator voltage and current waveforms are provided in Fig 13:

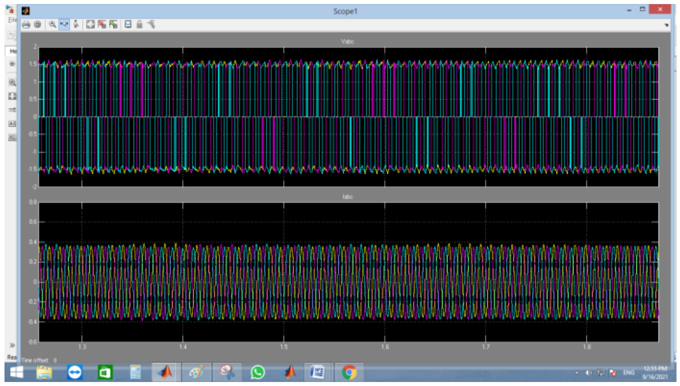

Fig 13 Stator Voltage and Current waveforms of PMSG based WECS

The dc voltage measured at the output side of machine side converter is provided below in Fig 14:

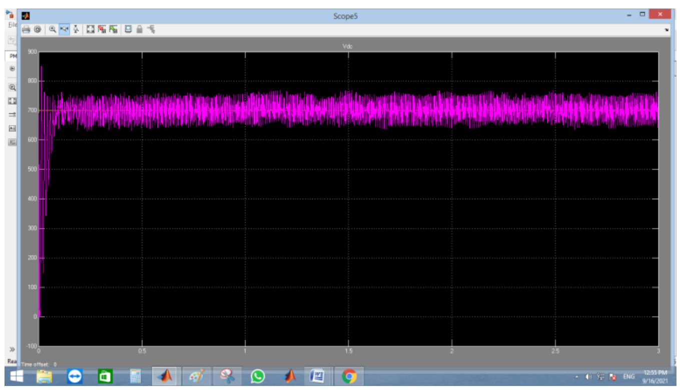

Fig 14 DC Link Voltage at MSC

In this, the dc voltage is controlled using the reference dc voltage of 700V provided to the controller. This is provided as the input of the buck converter. The buck converter steps down the voltage according to the load requirement. The load voltage and current is provided below in Fig 15:

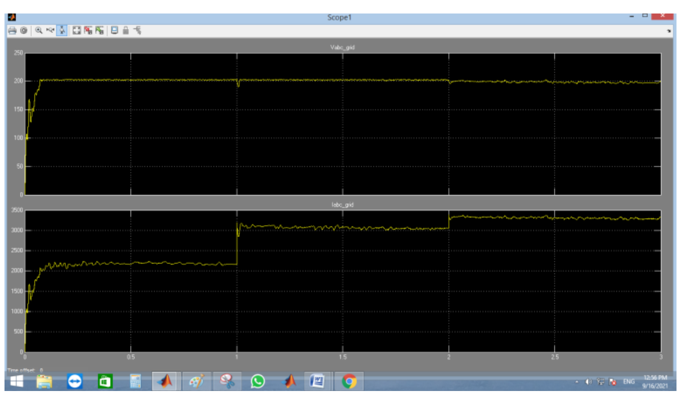

Fig 15 Load Voltage and Current Waveforms

In this, the load is increased at the time of 1s and 2s. Hence there is increase in current in those time periods and the voltage is maintained at 200V using the voltage mode control circuit or load side controller. The measured load voltage is around 202V for load1 and load2 and when load3 is connected, it is reduced to 196V which 2% reduced from the rated load voltage. The load power is provided in the following Fig 16:

Fig 16 Power Consumed by Load

As the load is increased at t=1s and 2s, the power consumption is also increased similar to current.

VII Conclusion

In this, multiple wind energy conversion system with PMSG is simulated along with Machine and load side converters. The controllers for these converters are also designed and voltage regulation at the load side is provided. ANN controller design is discussed and designed for the voltage mode control loop provided for load voltage regulation. The %regulation for the load is calculated as 98% for load3 and for other two loads, it is around 99%.

References

J. Zaragoza, J. Pou, A. Arias, C. Spiteri, E. Robles, and S. Ceballos, “Study and experimental verification of control tuning strategies in a variable speed wind energy conversion system,” Renewable Energy, vol. 36(5), pp. 1421-1430, 2011.

T. Ackermann, “Wind Power in Power System, West Sussex, England”: John Wiley and Sons, Ltd, 2005.

M. Mansour, M. N. Mansouri, M.F. Mmimouni, “Study and control of a variable-speed wind-energy system connected to the grid”, International Journal of Renewable Energy Research, vol. 1(2), pp. 96-104, 2011.

M. Cirrincione, M. Pucci, and G. Vitale, “Neural MPPT of variable speed wind generators with induction machines in a wide speed range ”, Proceedings in IEEE Conference on Energy Conversion Congress and Exposition, pp. 857-864, 2011.

A. K. Singh, R. Krisham, and Y. Sood, “Modeling and Control of Grid Connected Variable Speed PMSG Based Wind Energy System”, Conference on Advances in Communication and Control Systems 2013 (CAC2S 2013), Published by Atlantis Press.

B. Muhando, T. Senjyu, H. Kinjo, and T. Funabashi, “Extending the modelling framework for wind generation systems: RLS-based paradigm for performance under high turbulence inflow” IEEE Transactions on

Energy Conversion, vol. 24(1), pp. 211-221, 2009.

K. Tan, and S. Islam, “Optimum Control Strategies in Energy Conversion of PMSG Wind Turbine System without Mechanical Sensors”, IEEE Transactions on Energy Conversion, vol. 19(2) p392-399, June 2004.

L.G. Gonzalez, E. Figueres, G.Garcera, O.Carranza, “Modelling and control in wind energy conversion systems(WECS)” 13th European Conference on Power Electronics and Applications, EPE ,2009.

Y. Errami, M. Hilal, M. Benchagra, M. Ouassaid, M. Maaroufi, “Nonlinear Control Of MPPT and Grid Connected for Variable Speed Wind Energy Conversion System Based on the PMSG” Journal of Theoretical and Applied Information Technology, vol. 39(2), 2012.

Y. Errami, M. Ouassaid and M. Maaroufi, “Modelling and Control Strategy of PMSG Based Variable Speed Wind Energy Conversion System” International Conference on Multimedia Computing and Systems (ICMCS), 2011.

Wind, Reliability of Prototype Vertical Axis. "Design and Development of Permanent Magnet Synchronous Generator (Pmsg) Based on Svpwm Techniques Using Wind Ene..."International Journal of Electrical and Electronics Engineering Research (IJEEER) ISSN(P): 2250-155X; ISSN(E): 2278-943X 6.2, Apr 2016, 1-12

Saifee, A., and A. R. V. I. N. D. Mittal. "Design of novel axial flux permanent magnet generator (AFPMG) for wind energy applications." *Int J Electr Electr Eng Res* 4.3 (2014): 35-42.

Srikanth, KS, LV Narasimha Rao, and Vaddi Ramesh. "Improvement of Microturbine Generator Output Voltage Using Matrix Converter."International Journal of Electrical and Electronics Engineering Research (IJEEER) 4.2, Apr 2014, 319-326

Parmar, Jigar K., Sunny K. Darji, and Gajendra R. Patel. "Fuzzy Based MPPT Controller of Wind Energy Conversion System using PMSG." *International Journal of Electrical and Electronics Engineering (IJEEE)* 7.3: 17-30.